

On the estimation of body mass in temnospondyls: a case study using the large-bodied *Eryops* and *Paracyclotosaurus*

by LACHLAN J. HART^{1,2,*} , NICOLÁS E. CAMPIONE³  and MATTHEW R. MCCURRY^{1,2,4} 

¹Earth & Sustainability Science Research Centre, School of Biological, Earth and Environmental Sciences (BEES), University of New South Wales, Sydney, NSW 2052, Australia; l.hart@unsw.edu.au, m.mccurry@unsw.edu.au

²Australian Museum Research Institute, 1 William Street, Sydney, NSW 2010, Australia; lachlan.hart@australian.museum, matthew.mccurry@australian.museum

³Palaeoscience Research Centre, School of Environmental & Rural Science, University of New England, Armidale, NSW Australia; ncampion@une.edu.au

⁴Paleobiology, National Museum of Natural History, Smithsonian Institution, Washington, DC 20560, USA

*Corresponding author

Typescript received 14 March 2022; accepted in revised form 30 August 2022

Abstract: Temnospondyli are a morphologically varied and ecologically diverse clade of tetrapods that survived for over 200 million years. The body mass of temnospondyls is a key variable in inferring their ecological, physiological and biomechanical attributes. However, estimating the body mass of these extinct creatures has proven difficult because the group has no extant descendants. Here we apply a wide range of body mass estimation techniques developed for tetrapods to the iconic temnospondyls *Paracyclotosaurus davidi* and *Eryops megacephalus*. These same methods are also applied to a collection of extant organisms that serve as ecological and morphological analogues. These include the giant salamanders *Andrias japonicus* and *Andrias davidianus*, the

tiger salamander *Ambystoma tigrinum*, the California newt *Taricha torosa* and the saltwater crocodile, *Crocodylus porosus*. We find that several methods can provide accurate mass estimations across this range of living taxa, suggesting their suitability for estimating the body masses of temnospondyls. Based on this, we estimate the mass of *Paracyclotosaurus* to have been between 159 and 365 kg, and that of *Eryops* between 102 and 222 kg. These findings provide a basis for examining body size evolution in this clade across their entire temporal span.

Key words: Temnospondyli, amphibian, body mass estimation, allometry, *Eryops*, *Paracyclotosaurus*.

In extant organisms, body mass is strongly correlated with physiology and ecology (Gillooly *et al.* 2001; Brown *et al.* 2004). As such, determining the body mass of fossil taxa is of great interest to palaeontologists to elicit a better understanding of the ecology and evolution of extinct species (Burness *et al.* 2001; Codron *et al.* 2012; Benson *et al.* 2014, 2018; Grady *et al.* 2014; Schroeder *et al.* 2021). A variety of body mass estimation techniques have been applied to extinct vertebrates (see Campione & Evans 2020, and references therein) usually taking either a volumetric-density approach, using physical scale models or two- or three-dimensional digital reconstructions (Henderson 1999; Hurlbut 1999; Motani 2001; Hutchinson *et al.* 2007; Sellers *et al.* 2012; Brassey & Sellers 2014; Brassey *et al.* 2015, 2016; Witzmann & Brainerd 2017), or an extant-scaling approach (Anderson *et al.* 1985; Hurlbut 1999; Campione & Evans 2012; Campione *et al.* 2014; Campione 2017). Likewise, using general body size proxies based on physical measurements, such as

skull or limb-bone dimensions, snout–vent length (SVL) and total length (TL) to estimate the body masses of amphibians, birds, crocodilians and squamates, has been shown to provide accurate results in extant taxa and therefore applicable to closely related extinct taxa (Pough 1980; Farlow *et al.* 2005; Van Heteren *et al.* 2017; Santini *et al.* 2018). Despite moving towards a more unified framework for body mass estimation in fossil vertebrates (Campione & Evans 2020), there remain many questions about how broadly applicable various methods are across vertebrate groups, with only a few recent attempts to compare methods (Brassey 2017; Campione & Evans 2020; Rovinsky *et al.* 2020).

Temnospondyls are a large and diverse group of extinct amphibians. The preservation and mode of preparation of most temnospondyls do not allow the obtaining of some measurements required for certain body mass estimation techniques. For example, Campione & Evans's (2012) stylopodial regression (humeral and femoral least

2 PALAEONTOLOGY

circumferences; HcFc) estimation model for quadrupeds requires at least a humerus and femur, ideally from the same individual, preserved and prepared in three dimensions. Unfortunately, the fossils of many temnospondyls, especially Permian-aged taxa, are laterally or dorsoventrally flattened or prepared as panel mounts, limiting opportunities for measurement. Articulated or associated postcranial fossils of temnospondyls are generally rare. A similar problem is encountered when attempting two- or three-dimensional volumetric-density techniques. These methods are best-suited to working with complete or near-complete skeletons. Indeed, when employing graphic double integration to estimate the body mass of *Archegosaurus decheni*, Witzmann & Brainerd (2017) digitally reconstructed a skeleton based on several individuals. Furthermore, attempting to use equations based on measurements such as SVL or TL, as is common with extant amphibians (Pough 1980; Santini *et al.* 2018), also requires near-complete skeletal remains; an anteroposteriorly complete skull and presacral vertebral series are needed to measure SVL. Apart from the aforementioned study on *A. decheni*, which used graphic double integration (GDI), temnospondyls have not been included in body mass estimation studies.

The Permian eryopid temnospondyl *Eryops megacephalus* Cope, 1877, and the Triassic mastodonsaurid temnospondyl *Paracylotosaurus davidi* Watson, 1958, provide exceptions to the aforementioned problems. Both species are known from near-complete skeletons prepared in three dimensions. *Eryops megacephalus* is one of the most studied temnospondyls, the remains of which are common in Permian strata of the southwestern United States (see Pawley & Warren 2006, and references therein). Several *E. megacephalus* skeletons are on public display in museums globally. On the other hand, *P. davidi* is a single skeleton preserved in a large, fragmented ironstone nodule recovered from the Triassic (Anisian) Ashfield Shale and exposed in a brick pit in St Peters, Sydney, Australia, c. 1910. The skeleton of *P. davidi* is preserved within the nodule as a natural mould. Through the work of Mr F. O. Barlow over more than 40 years, plaster casts were created from artificial moulds made from the natural part and counterpart moulds left by the decayed bones in the ironstone. These casts were then reconstructed into the complete skeleton on which the original description was based (Watson 1958). At least two skeletons were produced from these moulds. The most well-known is on display at the Natural History Museum, London, UK, and the second is a formerly displayed cast at the Australian Museum, Sydney, Australia.

The near-complete skeletons and 3D preservation of *P. davidi* and *E. megacephalus* make them ideal cases to apply various body mass estimation methods and evaluate

their general applicability to Temnospondyli. Here, we apply extant-scaling and volumetric-density approaches to estimate the body masses of these two taxa and, to evaluate approach accuracy, we consider a selection of extant taxa hypothesized as morphologically or ecologically analogous to temnospondyls. We propose that our comparative context will provide a basis for accurately estimating the body mass of a vast number of temnospondyls, assuming the appropriate skeletal regions are preserved.

MATERIAL AND METHOD

Material

Institutional abbreviations. AM, Australian Museum, Sydney, Australia; AMNH, American Museum of Natural History, New York, USA; CR2P, The Center for Research on Palaeobiodiversity and Palaeoenvironments, Paris, France; FMNH, Field Museum, Chicago, USA; FSU, Friedrich Schiller University, Jena, Germany; MNHN, Muséum national d'Histoire naturelle, Paris, France; NHM (BMNH), Natural History Museum, London, UK (PV refers to the Vertebrate Palaeontology Collection); NHMW, Naturhistorisches Museum, Vienna, Austria; THNC, Texas Memorial Museum, Austin, Texas, USA; NENH, Natural History Museum, University of New England, Armidale, New South Wales, Australia; UT, University of Texas, Austin, USA.

Selection of extant analogues. Establishing an appropriate modern analogue for temnospondyls is complicated, as temnospondyls are morphologically and possibly ecologically distinct from modern amphibians. There is much discussion around the phylogenetic history of temnospondyls, their relationship among early tetrapods, and the origins of Lissamphibia (Milner 1988; Trueb & Cloutier 1991; Milner 1993; Witmer 1995; Laurin & Reisz 1997, 1999; Schoch & Milner 2004; Ruta & Coates 2007; Marjanović & Laurin 2013; Atkins *et al.* 2019; Schoch 2019). However, even if extant phylogenetic homologues to temnospondyls were to be established, these may not provide accurate morphological or ecological analogues due to the myriad forms and inferred ecologies of the group (e.g. Fortuny *et al.* 2011). As there is no single living taxon unambiguously analogous to temnospondyls, a selection of extant taxa is required that are ecologically (with similar life modes) and morphologically comparable to temnospondyls. Of the three living clades of amphibians, salamanders (Caudata) share the most morphological similarities to temnospondyls (including their limb dimensions and presence of a tail), and so, where available, linear equations based on salamanders are used herein.

Many temnospondyls exhibit a much larger and more robust skull relative to their body than extant salamanders. These large skulls and elongated snouts draw superficial comparisons with crocodyliforms (Damiani 2008). Due to this crocodile-like skull shape and the proportions of the body, the ecology of this group of temnospondyls has also been inferred to be analogous to modern crocodiles (Chernin 1970), that is, as semi-aquatic ambush predators. Therefore, we have also included several linear equations based on extant crocodilians, including skull width and length, and measurements of the femur.

As the two temnospondyls in this study are examples of either primarily terrestrial (*Eryops megacephalus*) or aquatic (*Paracyclotosaurus davidi*) taxa (although both are inferred to have semi-aquatic tendencies; Sulej & Majer 2005; Schoch 2009), extant comparative taxa were chosen to reflect these ecologies. These analogues include obligately aquatic (*Andrias japonicus* and *Andrias davidianus*) and terrestrial (*Ambystoma tigrinum*) salamanders, and two semi-aquatic taxa: a newt (*Taricha torosa*) and a crocodilian (*Crocodylus porosus*).

FMNH 31536 is a preserved wet specimen of *Andrias japonicus*. A three-dimensional mesh of the skeleton of FMNH 31536 was acquired through MorphoSource (<https://doi.org/10.17602/M2/M77893>). The mesh (Fig. 1A) was produced from a computed tomography (CT) scan (scanned with a General Electric phoenix v|tome|x s, at UChicago PaleoCT, University of Chicago, using 120 V and 134 A, obtaining X and Y pixel spacing of 0.5221 mm, and Z pixel spacing of 0.335 mm; Hart (2022a, 2022b)). The tail of this specimen was straightened using Artec Studio 15 (Artec Group, Inc; <https://www.artec3d.com>). The wet weight, total length (TL) and snout–vent length (SVL) of FMNH 31536 were measured manually, with a scale and tape measure, and provided to us by Daryl Coldren and Joshua Mata (FMNH). The effects of preservation on the weight of this specimen were considered; Pierson *et al.* (2020) reported up to 40% mass loss in preserved salamanders, so a weight range of 7.70–12.83 kg was calculated accordingly. The remaining measurements were derived from the three-dimensional mesh in MeshLab v2020.12 (ISTI-CNR; <https://www.meshlab.net>).

Specimen stock no. 1/2009 is a specimen of *Andrias davidianus* housed at the Zoological Collection of the Department of Theoretical Biology, University of Vienna, Austria. We used a three-dimensional mesh (Fig. 1C) of this specimen (<https://doi.org/10.17602/M2/M446021>) previously used in other studies (Heiss *et al.* 2013; Fortuny *et al.* 2015), derived from a CT scan (scanned with a Somatom emotion medical multi-slice CT scanner (Siemens AG, Germany) at the Clinic of Diagnostic Imaging University of Veterinary Medicine Vienna (Austria) using

130 kV, 100 mA, obtaining 0.725 mm of pixel size and an output of 512 × 512 pixels per slice with an interslice space of 0.4 mm (Fortuny *et al.* 2015)). The three-dimensional reconstruction and segmentation were performed in Avizo 7.0 (VSG, Germany; <https://www.thermofisher.com/au/en/home/electron-microscopy/products/software-em-3d-vis/3d-visualization-analysis-software.html>, see Heiss *et al.* 2013). The specimen is missing a portion of the tail, reconstructed in Artec Studio 15 (Artec Group, Inc; <https://www.artec3d.com>) with the tail from the *A. japonicus* scan above. All measurements were taken in MeshLab v2020.12 (ISTI-CNR). As the actual weight of this specimen is unknown (TL 1270 mm), mass ranges for *A. davidianus* were obtained from the literature of 25–50 kg (Liu 1950; Browne *et al.* 2014) based on specimens between 1056 and 1800 mm TL.

Computed tomography scans of both *Ambystoma tigrinum* (THNC 17991) and *Taricha torosa* (THNC 19196) were obtained from <http://digimorph.org> (Digimorph Staff 2008a, 2008b; CC BY-NC 4.0) (Fig. 1E, G). Both specimens are from the collections of the Texas Memorial Museum. Specimens were scanned by Matthew Colbert (UT) at The University of Texas High-Resolution X-ray CT Facility on 28 September 2007. The coronal axis contains a total of 1528 slices. Each 1024 × 1024 pixel slice is 0.08342 mm thick, with an interslice spacing of 0.08342 mm and a field of reconstruction of 35 mm (Digimorph Staff 2008a, 2008b). Data were segmented using Dragonfly software, v2021.1 for Windows (ORS; <http://www.theobjects.com/dragonfly>) and three-dimensional surface meshes were generated. The meshes were measured in MeshLab v2020.12 (ISTI-CNR). Body masses for both taxa were derived from the literature (Latimer *et al.* 1961; Feder 1978) based on average masses for similarly sized representatives of each species (0.022–0.045 kg for *A. tigrinum*, 0.0073–0.0140 for *T. torosa*).

NENH-RE-00266 (formerly XCb Cp4) is a sub-adult *Crocodylus porosus* in the collection of the Natural History Museum of the University of New England, Armidale, Australia. A mesh (Fig. 1I) derived from the CT scan of NENH-RE-00266 (<https://doi.org/10.17602/M2/M446000>) previously used by Klinkhamer *et al.* (2017), was measured in MeshLab v2020.12 (ISTI-CNR) (CT scans were taken on a Siemens Syngo CT2012B, scan data contained 3019 slices at 120 kV and a slice thickness of 0.75 mm, and CT data were analysed in Mimics v16.02; Materialise; <https://www.materialise.com>). A mass range for NENH-RE-00266 (TL 2100 mm) was derived from the literature (Seymour *et al.* 2013 recorded a sub-adult *C. porosus* specimen with TL 2189 mm to have a mass of 43.4 kg; Klinkhamer *et al.* 2017 estimated the mass of NENH-RE-00266 to be 25–30 kg). Measurements of all taxa are summarized in Table 1.

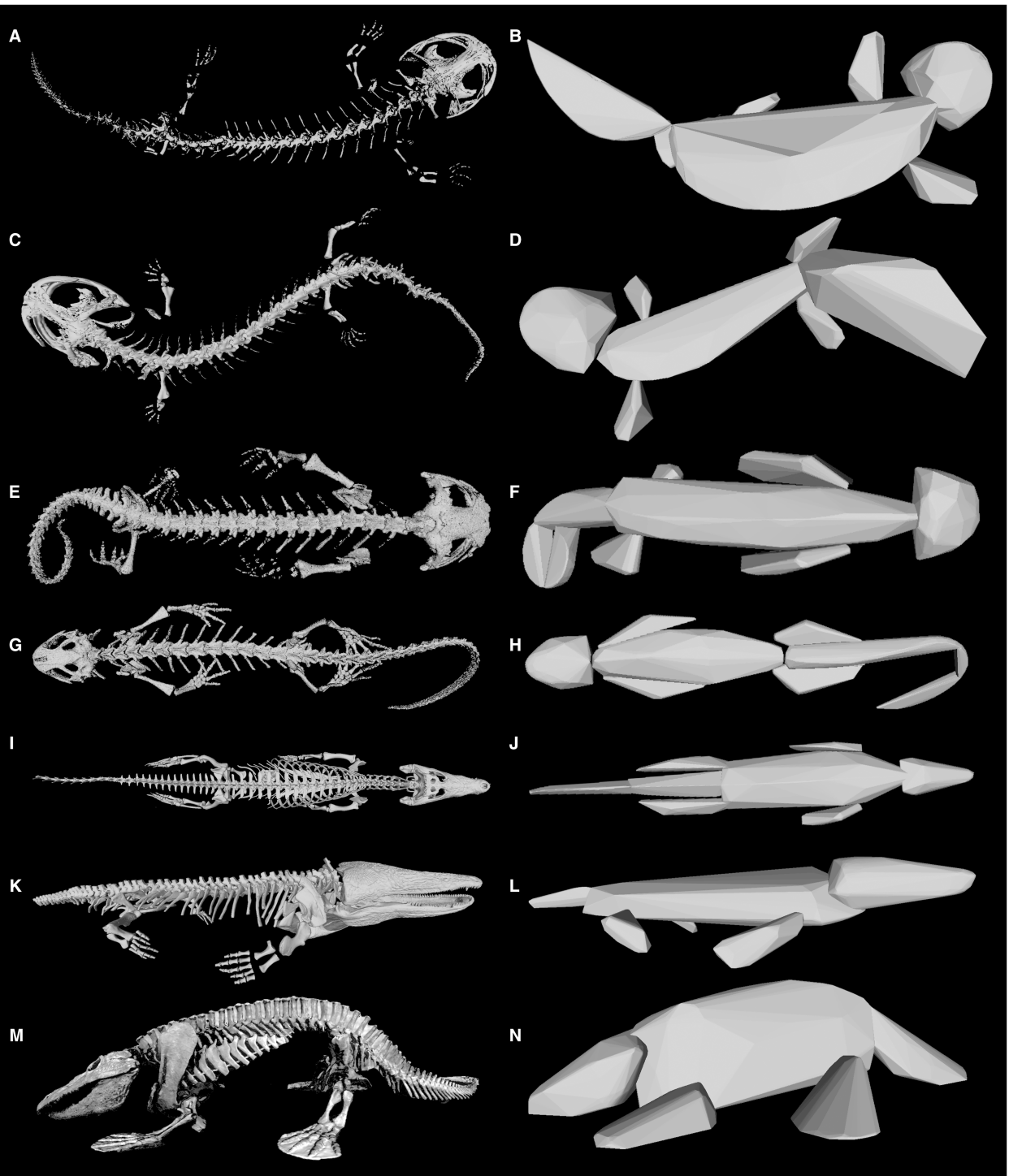


FIG. 1. Included taxa, three-dimensional skeletal models (A, C, E, G, I, K, M) and convex hull models (B, D, F, H, J, L, N); A–B, *Andrias japonicus*, FMNH 31536. C–D, *Andrias davidianus*, NHMW specimen stock no. 1/2009. E–F, *Ambystoma tigrinum*, THNC 17991. G–H, *Taricha torosa*, THNC 19196. I–J, *Crocodylus porosus*, UNE NENH-RE-00266. K–L, *Paracyclotosaurus davidi*, AM F151922. M–N, *Eryops megacephalus*, MNHN-F-1957-6.

Fossil specimens. AM F151922 is a cast of *Paracyclotosaurus davidi*, based on the holotype BMNH PV R 6000. A three-dimensional model of AM F151922 was generated

by surface scanning each skeletal element with an Artec Spider EVA-S 3D scanner (Fig. 1K; <https://doi.org/10.17602/M2/M445991>). The surface scans of the elements

TABLE 1. Measurements of included taxa (in mm).

	<i>Paracyclotosaurus davidi</i>	<i>Eryops megacephalus</i>	<i>Andrias japonicus</i>	<i>Andrias davidianus</i>	<i>Ambystoma tigrinum</i>	<i>Taricha torosa</i>	<i>Crocodylus porosus</i>
TL	2450	1920	1030	1270	172	163	2100
SVL	1660	1000	595	855	90	72	1044
FC	96	102	30	40	4	4	53
HC	125	122	24	35	6	5	50
HFC	221	224	54	74	11	9	103
FL	215	177	44	63	10	10	142
Fdw	75	48	18	24	3	3	31
Fdh	45	51	8	11	2	3	16
Fpmx	81	51	14	20	2	2	26
Fpmn	66	40	8	12	2	2	19
Ftr	95	86	12	18	2	2	56
HW	354	305	118	170	20	12	154
HL	600	354	104	180	20	15	281

Abbreviations: FC, femoral circumference; Fdh, femur distal height; Fdw, femur distal width; FL, femur length; Fpmn, minimum diameter of proximal end of femur; Fpmx, maximum diameter of proximal end of femur; Ftr, distance from proximal end of femur to fourth trochanter; HC, humeral circumference; HFC, combined humeral and femoral circumference; HL, head length; HW, head width; SVL, snout–vent length; TL, total length.

were fused digitally in Artec Studio 15 (Artec Group, Inc; <https://www.artec3d.com>). All measurements were derived from the three-dimensional model using MeshLab v2020.12 (ISTI-CNR).

MNHN-F-1957-6 is a high fidelity cast of AMNH FARB 4657, *Eryops megacephalus*. AMNH FARB 4657 is a near-complete, mounted skeleton on *E. megacephalus*. A three-dimensional photogrammetry model (<https://doi.org/10.17602/M2/M445996>) of MNHN-F-1957-6 created by Lilian Cazes (CR2P, MNHN) in 2014 was used in this study (Fig. 1M). The model was constructed from 288 photographs taken with a Canon 5D Mark II camera with an EF 24–105 mm F/4 lens. Photographs were processed in Photoshop CC 2014, and the reconstruction was created in Photoscan (Metashape) v1.1.0 (Agisoft; <https://agisoft.com>). Physical measurements of the skull length (SKL) were taken to scale the specimen appropriately. All other measurements of MNHN-F-1957-6 herein were obtained from the photogrammetric model in MeshLab v2020.12 (ISTI-CNR).

Methods

Graphic double integration. Silhouettes of all seven taxa were created based on lateral and dorsal views of the three-dimensional skeletal meshes. The extent of soft tissue surrounding the skeletons was reconstructed based on comparisons with living examples of the extant taxa (following Witzmann & Brainerd 2017). Pixel measurement of these silhouettes was carried out in GIMP v2.10.8 (<https://www.gimp.org>). Here, lines were drawn across

the lateral and dorsal silhouettes (effectively creating dorsal and lateral cross-sections), and the number of pixels for each was recorded. Using the perpendicular vertical and transverse lines represent the diameters (d_v and d_t respectively) of each slice, the area of each ellipse (A_e) (in pixels²) was calculated as:

$$A_e = \frac{\pi d_v d_t}{4}$$

The average of all elliptical areas (\bar{x}) (the number of which differed for each taxon, depending on the size of the silhouette) was then calculated and multiplied by the total length (in pixels), providing an approximate measure of the volume of the silhouetted region (B_v) (in pixels³):

$$B_v = \bar{x} \cdot TL$$

This method was repeated for the fore and hind limbs and doubled to account for paired limbs (FL_v) and (HL_v). The volume estimates were then scaled by dividing the length of the image in pixels by the total length of the specimen (in cm). These were added together to generate an estimate for the entire body:

$$M = B_v + FL_v + HL_v$$

Three estimates were generated to accommodate for variable body density assumptions. For the extant taxa, this included the raw estimate above (calculated assuming a neutral specific gravity of 1.0) and a second estimate based on the specific gravity of amphibians (1.05 for the salamanders) or crocodiles (1.06 for *C. porosus*) as

outlined by Larramendi *et al.* (2020). The median of the two estimates above was calculated to generate a ‘mid’ estimate for the extant taxa. For the temnospondyls, the specific gravities of amphibians and crocodiles were both applied to the volume estimate, which, combined with the uncorrected estimate (assuming a specific gravity of 1.0), served to provide lower, middle and upper estimates.

Convex hull. The three-dimensional meshes of each specimen were split into functional elements, including the head, trunk, forelimb, hindlimb and tail regions using MeshLab v2020.12 (ISTI-CNR). The tail was divided into sections for skeletons with curved tails. Each element was converted to a convex hull polygon using Meshlab’s ‘Convex Hull’ function (Fig. 1B, D, F, H, J, L, N) and saved as a point cloud. The point cloud was imported into MATLAB vR2021a (The Mathworks Inc; <https://www.mathworks.com/products/matlab.html>), and the minimum convex hull (MCH) volume was calculated using the ‘convhull’ command. An additional convex hull estimate was generated for each of the four salamanders, employing a model which incorporated the head and body as a single functional element, instead of two separate elements. This was done to simulate the appearance of the animal in life. For the extant taxa, volumes were converted to mass by multiplying volumes by the specific gravity calculated by Larramendi *et al.* (2020) for amphibians and crocodiles. The temnospondyls were calculated using the specific gravity of crocodiles. The minimum convex hull volumes for each body region were summed and the total multiplied by 1.091, 1.206, and 1.322 (as per the 95% confidence interval (CI) of Sellers *et al.* 2012) to generate lower, mean and upper body mass estimates, respectively.

Extant-scaling. Four extant-scaling algorithms originally devised for extant salamanders were applied (Pough 1980; Santini *et al.* 2018). The anteroposterior length from the end of the rostrum to the sacrum was used as an osteological correlate for SVL, as the exact location of the cloaca cannot be obtained from skeletons. Pough’s second formula uses TL as the independent variable (see Pough 1980 for formulae). Santini *et al.* (2018) developed two length-to-mass scaling equations for salamanders, also using SVL, for paedomorphic and non-paedomorphic taxa (see Santini *et al.* 2018 for formulae). The mean absolute percentage error (MAPE) of these formulae, given by Santini *et al.* (2018), is 44.792%. This error was applied to all mass estimates based on Santini’s model to generate upper and lower error bounds.

Crocodyliform body mass has historically been estimated using several methods (see O’Brien *et al.* 2019 and

references therein) that primarily focus on cranial or femoral dimensions. O’Brien *et al.* (2019) provided an extant-scaling equation for predicting body mass based on head width (HW) (see O’Brien *et al.* 2019 for details). Upper and lower estimates were calculated using the error of 0.193, as given by O’Brien *et al.* (2019). As this model was based on captive crocodylians only, O’Brien *et al.* (2019) applied a 25% mass correction to all estimates, to compensate for the discrepancy between captive and wild crocodylians. Here, we also generated a second set of estimates by reducing our raw results by 25%, following the methodology of the original study.

Farlow *et al.* (2005) outlined a range of measurements based on the femur of *Alligator mississippiensis* to create growth trajectories for estimating the mass of extinct mesoeucrocodylians. In our study, we use the equations based on femur length (FL), femur distal width (Fdw), femur distal height (Fdh), maximum diameter of proximal end of femur (Fpmx), minimum diameter of proximal end of femur (Fpmn), femoral minimum midshaft circumference (Fc), and distance from proximal articular end to fourth trochanter (Ftr). We followed the method outlined in Farlow *et al.* (2005, fig. 2), to make these measurements. Furthermore, Farlow *et al.* (2005) also gave regression equations for TL and head length (HL) and a multivariate equation (which uses Ftr and FL). Refer to Farlow *et al.* (2005) for all formulae.

Finally, the body masses of included taxa were calculated using the stylopodial regression formula of Campione & Evans (2012), calculated using the QE function within the R v4.0.4 (R Core Team 2013) package MASSTIMATE v2.0-1 (Campione *et al.* 2014; Campione 2020), wherein lower and upper estimates were also generated, based on a 25% percentage prediction error (PPE). PPE was calculated using the PE function in the MASSTIMATE package v2.0-1 (Campione *et al.* 2014; Campione 2020).

RESULTS

Extant taxa

Across all five extant taxa, the 25% corrected crocodylian HW allometric equation (O’Brien *et al.* 2019) provided body mass estimations consistently close to the actual masses outlined above (Figs 2–4). O’Brien *et al.*’s (2019) uncorrected crocodylian HW equation also provided accurate body mass estimates for the extant taxa (Figs 2–4), although the upper ranges were slightly higher than expected for these taxa. O’Brien’s (2019) equations produced the two narrowest ranges of PPE and were among the lowest PPE (Fig. 5).

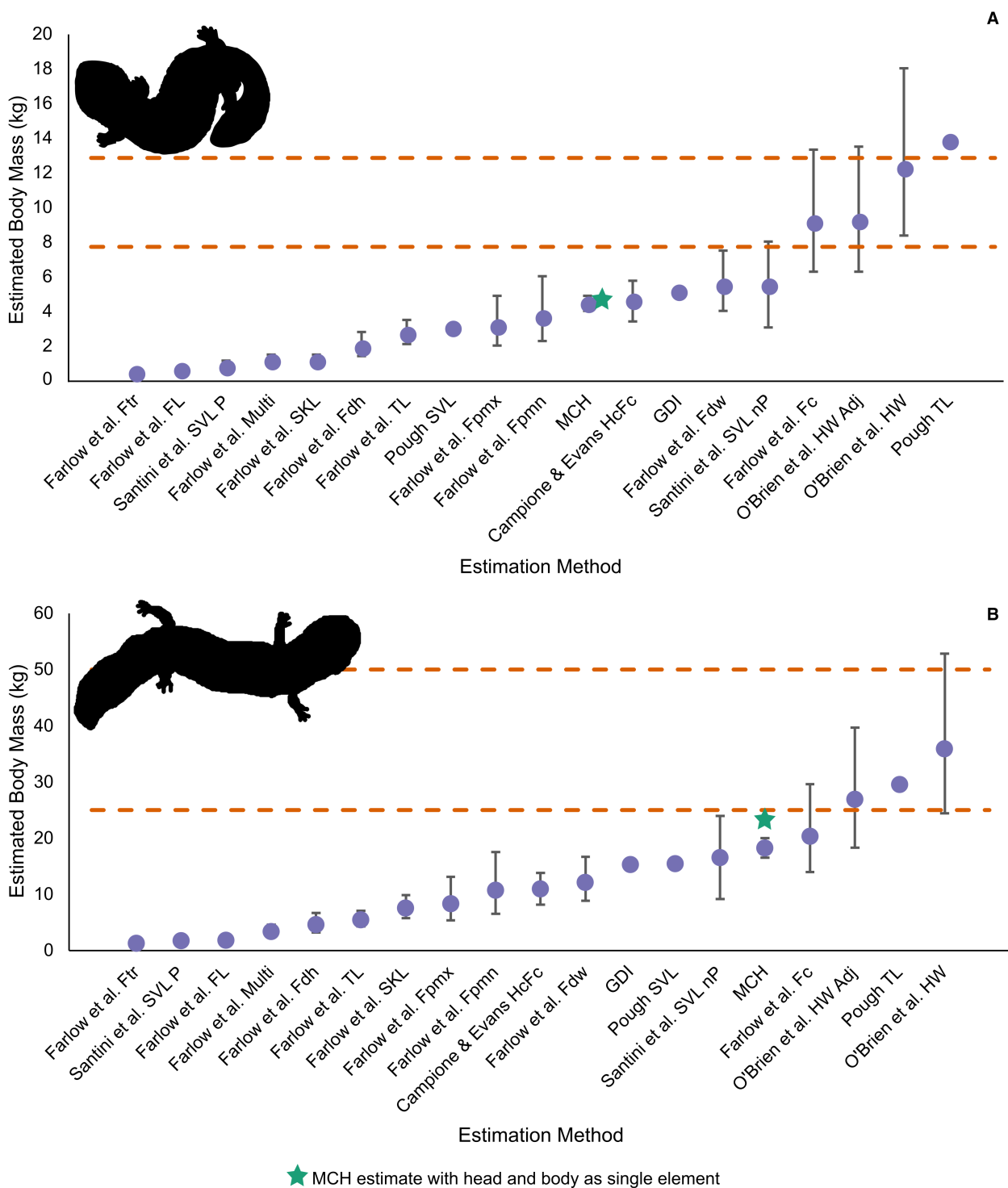


FIG. 2. Results of applied body mass estimation methods: A, *Andrias japonicus*; B, *Andrias davidianus*. See text for details of error ranges and individual estimation methods. Dashed lines indicate known mass range; for sources see text. Stars indicate mass estimation based on alternate MCH model of combined head and body. Silhouette image of *A. japonicus* from Phylopic (<http://phylopic.org>; Y. de Hoeve; vectorized by T. Michael Keesey; CC0 1.0).

Pough's (1980) TL allometric equation (developed for salamanders) produced mass estimates that align with the observed masses of the salamanders included in this study

(Figs 2, 3). The estimate for *Crocodylus porosus* (Fig. 4) is extremely high (184 kg) compared to the estimates generated by other methods and the actual mass of the animal

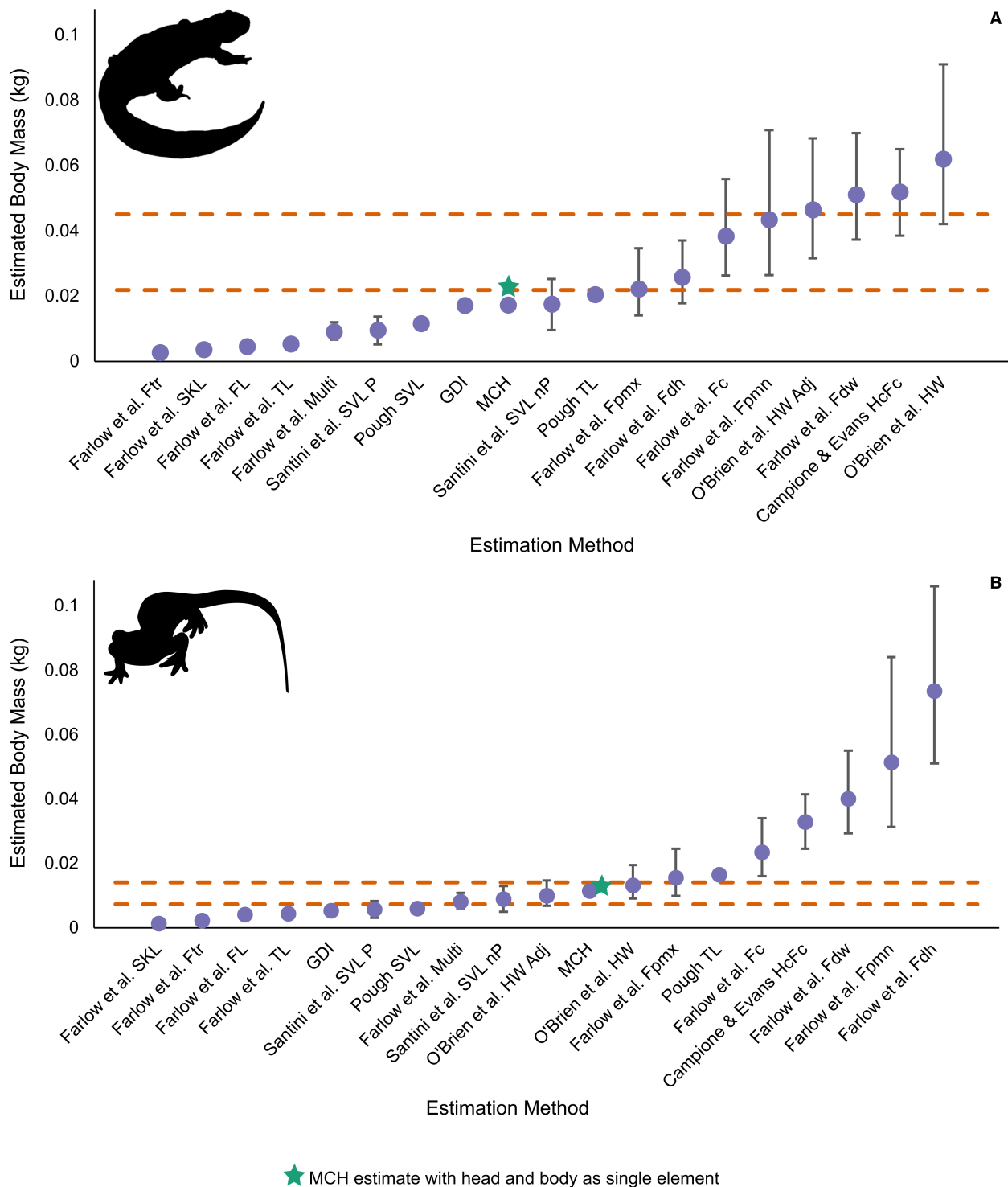


FIG. 3. Results of applied body mass estimation methods: A, *Ambystoma tigrinum*; B, *Taricha torosa*. See text for details of error ranges and individual estimation methods. Dashed lines indicate known mass range; for sources see text. Stars indicate mass estimation based on alternate MCH model of combined head and body. Silhouette images from Phylopic (<http://phylopic.org>: *A. tigrinum*, Matt Reinbold (modified by T. Michael Keesey), CC BY-SA 3.0); *T. torosa*, Neil Kelley, CC0 1.0).

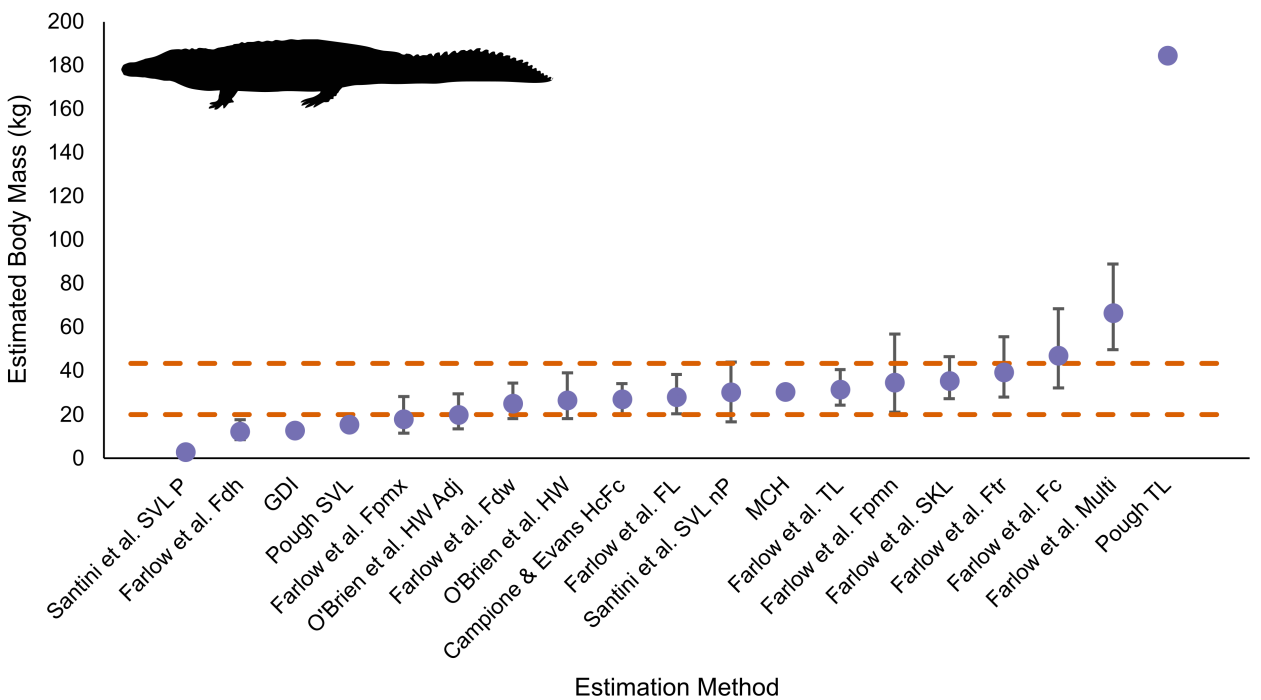


FIG. 4. Results of applied body mass estimation methods for *Crocodylus porosus*. See text for details of error ranges and individual estimation methods. Dashed lines indicate known mass range; for sources see text. Silhouette image from Phylopic (<http://phylopic.org>; *C. porosus*, Smokeybjb, CC BY-SA 3.0).

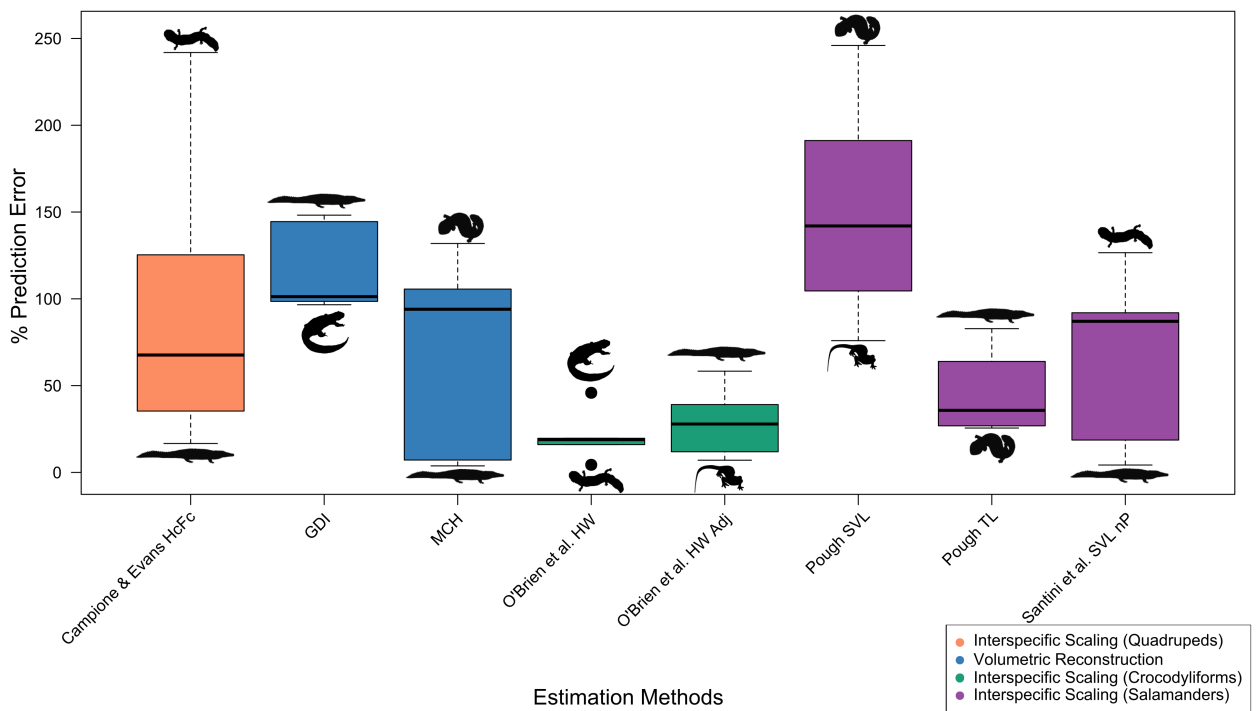


FIG. 5. Percentage prediction error (PPE) of eight selected models from this study. Silhouettes indicate outlier taxa for each method. Silhouette images from Phylopic (<http://phylopic.org>): *A. japonicus*, Y. de Hoev; vectorized by T. Michael Keesey, CC0 1.0; *A. tigrinum*, Matt Reinbold (modified by T. Michael Keesey), CC BY-SA 3.0; *T. torosa*, Neil Kelley, CC0 1.0; *C. porosus*, Smokeybjb, CC BY-SA 3.0.

in life. Pough's (1980) SVL equation produced estimates lower than the actual masses of all extant taxa.

Farlow *et al.*'s (2005) FC equation generated 16–34 g estimates for *T. torosa* and 32–69 kg for *C. porosus*. Both estimates are higher than the actual mass ranges for these taxa. Conversely, this same equation produced accurate estimations of the mass of *A. japonicus*, *A. davidianus* and *A. tigrinum*, of 6–13 kg, 14–30 kg and 26–56 g, respectively (Figs 2, 3A). All other methods developed by Farlow *et al.* (2005) did not provide consistently accurate estimates when applied to all extant taxa: Fdw proved accurate for *A. tigrinum* and *C. porosus*; Fpmn for *A. tigrinum* and *C. porosus*; Fdh for *A. tigrinum* only; Fpmx for *A. tigrinum*, *T. torosa* and *C. porosus*, Ftr, SKL, TL and FL for *C. porosus* only, and the multivariate equation for *T. torosa* only (Figs 2–4).

Campione & Evans' (2012) HcFc stylopodial regression equation produced an accurate estimate (20–34 kg) for *C. porosus* (Fig. 4). This method underestimated the masses of both *Andrias* species (3–6 kg for *A. japonicus*; 8–14 kg for *A. davidianus*) and overestimated the smaller salamanders (38–65 g for *A. tigrinum* and 24–41 g for *T. torosa*). Although this equation produced the widest PPE range (Fig. 5), this is largely due to *A. davidianus* as a single outlier. The mean PPE of Campione & Evans' (2012) is less than that of both GDI and Pough (1980) SVL.

Convex hull estimates (MCH) were lower than expected in *Andrias davidianus*, *A. japonicus* and *A. tigrinum* (16–20 kg, 4–5 kg and 16–19 g, respectively) but accurate for both *T. torosa* (10–13 g) and *C. porosus* (28–34 kg; Figs 2–4). The MCH estimate for *C. porosus* is very similar to that which was generated by many other methods used herein (O'Brien *et al.* 2019 HW; Farlow *et al.* 2005 Fpmn, SKL, TL and FL; and Campione & Evans 2012 HcFc; Fig. 4). MCH estimates included the widest range of PPE, disregarding outliers (Fig. 5). The second MCH estimates, applied to the four salamander taxa, which considered the head and body as a single functional element rather than two separate units, provided similar estimates to the above in *A. japonicus* (Fig. 2A), *A. tigrinum* (Fig. 3A) and *T. torosa* (Fig. 3B). In *A. davidianus*, the estimate produced was considerably higher (24 kg) and much closer to the actual mass of the animal in life (>25 kg).

Santini *et al.*'s (2018) SVL nP (non-paedomorphic) equation underestimated the mass in all extant taxa except *T. torosa* (5–13 g) and *C. porosus* (17–44 kg; Figs 3B, 4). Santini *et al.*'s (2018) SVL P (paedomorphic) equation produced very low mass estimates in all extant species.

In all extant taxa (Figs 2–4), the GDI method produced low body mass estimates. For *A. japonicus* (5 kg), *A. davidianus* (15–16 kg), and *C. porosus* (12–13 kg), these estimates are substantially lower than the mass of each taxon in life. The estimates for *A. tigrinum* (16–17 g) and *T. torosa* (5 g), although also underestimated, are closer to the actual mass of each taxon.

Fossil taxa

The O'Brien *et al.* (2019) 25% corrected method produced estimates in the ranges of 160–346 kg for *P. davidi* (Fig. 6A) and 103–223 kg for *E. megacephalus* (Fig. 6B). When O'Brien *et al.*'s (2019) uncorrected equation was applied to *P. davidi* (Fig. 6A) and *E. megacephalus* (Fig. 6B), estimates in the ranges of 213–461 kg and 137–297 kg were generated, respectively.

When applied to *E. megacephalus*, Pough's (1980) TL equation produced an estimate (133 kg) that is not dissimilar to the adjusted O'Brien *et al.* (2019) HW estimate (Fig. 6B) above. The estimate produced for *P. davidi* (323 kg) is slightly higher than those produced by most other methods in this study (Fig. 6A). Pough's (1980) SVL equation produced mass estimates of 61 kg for *P. davidi* and 24 kg for *E. megacephalus*. Both estimates are considerably lower than those generated by other equations in this study.

Farlow *et al.*'s (2005) equations provided a wide range of mass estimations for the temnospondyls, ranging from 42–69 kg (TL equation) to 599–1607 kg (Fpmn equation) for *P. davidi*, and from 18–30 kg (TL equation) to 228–474 kg (Fdh equation) for *E. megacephalus*. Of note is the FC equation, which, when applied to *P. davidi*, gives a mass estimation of 172–365 kg, which is similar to those produced by the O'Brien *et al.* (2019) and Pough (1980) methods (Fig. 6A). However, the same formula applied to *E. megacephalus* produces a mass estimate (205–434 kg) considerably higher than most other methods applied here.

Campione & Evans' (2012) equation, when applied to *P. davidi*, provided an estimated mass (163–276 kg) within the range of both O'Brien *et al.*'s (2019) adjusted HW and Farlow *et al.*'s (2005) FC (Fig. 6A). The estimate produced for *E. megacephalus* (169–286 kg) is relatively high compared to most other methods applied here (Fig. 6B).

When calculated for *P. davidi* and *E. megacephalus* (Fig. 6), the MCH estimates (220–267 and 106–128 kg, respectively) do not differ greatly from the estimates generated using O'Brien *et al.*'s (2019) adjusted and non-adjusted HW allometries, or Pough's (1980) TL allometry. Additionally, the MCH estimate for *P. davidi* is also very similar to that produced by Farlow *et al.*'s (2005) FC equation and Campione & Evans' (2012) HcFc stylopodial regression equation (Fig. 6A).

When applied to *P. davidi* and *E. megacephalus* (Fig. 6), the estimates derived from Santini *et al.*'s (2018) SVL nP (non-paedomorphic) equation (69–181 kg and 27–70 kg, respectively) are lower than those produced by most other methods used here. Santini *et al.*'s (2018) SVL P (paedomorphic) equation generated the lowest of all estimates of the fossil taxa with 5–12 kg for *P. davidi* and 2–12 kg for *E. megacephalus*.

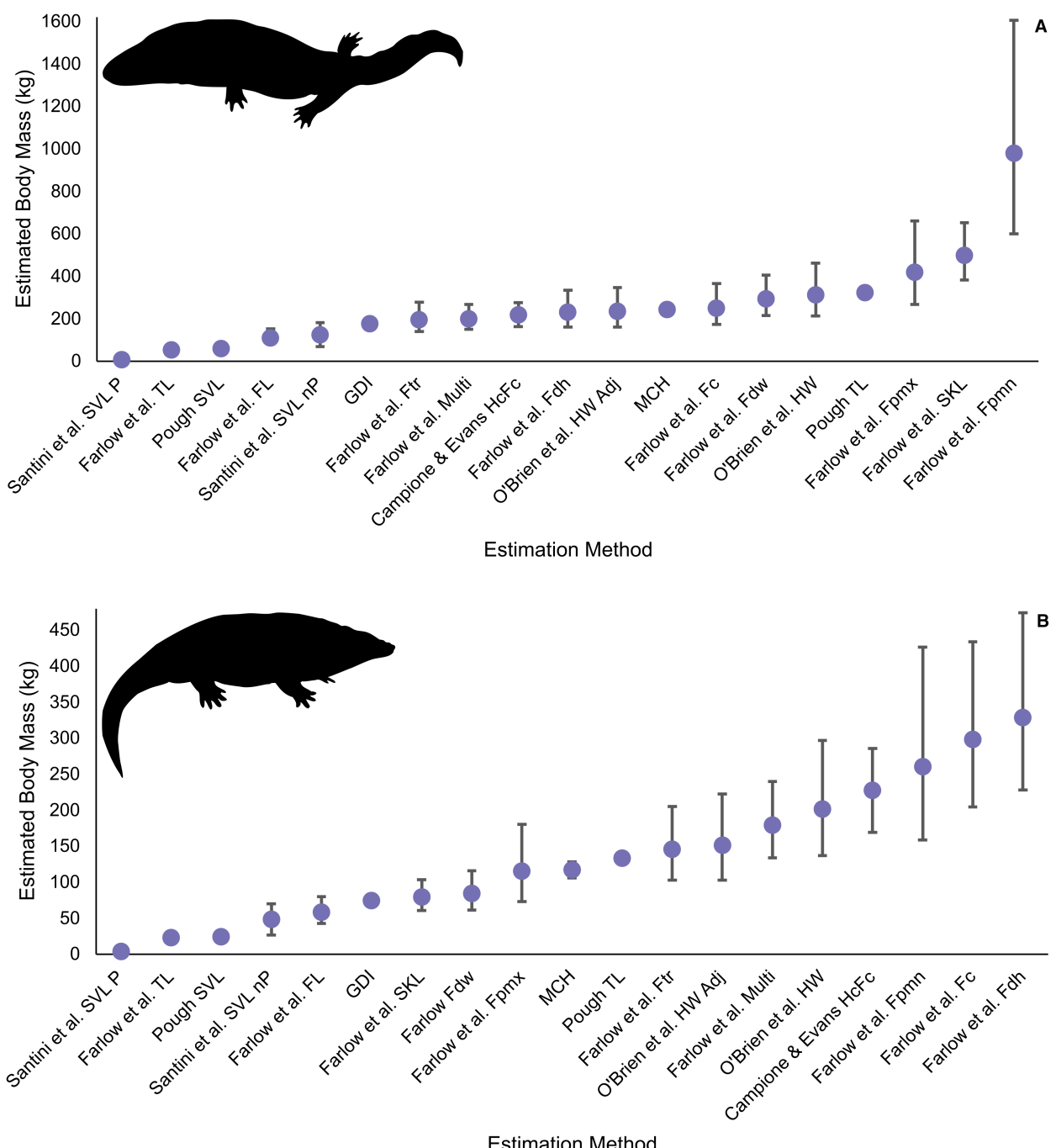


FIG. 6. Results of applied body mass estimation methods for extinct taxa: A, *Paracyclotosaurus davidi*; B, *Eryops megacephalus*. See text for details of error ranges and individual estimation methods. Silhouette images from Phylopic (<http://phylopic.org>): *P. davidi*, Dmitry Bogdanov (vectorized by T. Michael Keesey), CC BY 3.0; *E. megacephalus*, Dmitry Bogdanov (vectorized by T. Michael Keesey), CC BY-SA 3.0.

The GDI estimates produced for the temnospondyls are lower than most of those produced by the other methods in this study (Fig. 6), with *P. davidi* being estimated at 169–179 kg and *E. megacephalus* at 71–75 kg.

DISCUSSION

Estimating the body mass of extinct taxa is of key importance for understanding their biological and ecological

attributes. We assessed various methods for estimating mass in temnospondyls. These approaches are not without limitations, but by comparing a broad array of methods, we aimed to identify appropriate approaches to use in future work. Although the methods generated widely different results, four methods (HW, TL, stylopodial circumference (HcFc) and MCH) consistently produced accurate mass estimations of the extant taxa.

The accuracy of O'Brien *et al.*'s (2019) HW method was unexpected, given that it was developed specifically for crocodyliforms (Figs 2, 3). It is plausible that this accuracy is related to the shared ecology of these taxa, or potentially to discrete morphological similarities such as dorsoventrally low skulls (possibly a convergent morphology due to their aquatic habits). Accepting this caveat (that the model was generated for use with crocodyliforms), the estimates for *Paracyclotosaurus davidi* (220–267 kg) and *Eryops megacephalus* (102–222 kg) appear to be reasonable, based on the relative size of these taxa compared to extant animals of similar length. For example, the Hawaiian monk seal (*Monachus schauinslandi*) reaches lengths comparable to *P. davidi* (Reif *et al.* 2004), and has a similar mass to the estimate derived for *P. davidi* above (Smith *et al.* 2003). Likewise, *E. megacephalus* has a total length similar to the pygmy hippopotamus (*Choeropsis liberiensis*) and the above mass estimation also falls within a range akin to that of *C. liberiensis* (Flacke & Decher 2019). These comparisons are included accepting the limitations that *M. schauinslandi* and *C. liberiensis* are both mammals with very specific adaptations: a highly insulated body adapted for diving, and a graviportal form with a reduced tail, respectively.

There are undoubtedly some cases in which using the width of the skull would not be appropriate to estimate the body mass of temnospondyls. For example, the pliosaurid *Gerrothorax pulcherrimus* has a relatively wide skull (roughly 340 mm, see Jenkins *et al.* 2008) compared to the rest of its body (Schoch & Witzmann 2012). Applying O'Brien's (2019) equation to this taxon gives an estimate of 189–409 kg, which is unreasonably high for an animal whose total length probably did not exceed 1 m. There are also cases where using skull width would be impractical, where the skull is incomplete or is missing entirely. In these situations, using methods such as Campione & Evans' (2012) HcFc or Pough's (1980) TL equations may be more appropriate.

When applied to *E. megacephalus*, Pough's (1980) TL equation produces an estimate of 133 kg, well within the aforementioned range, whereas the estimate generated for *P. davidi* is slightly higher (323 kg). We suggest that Pough's method may be useful in estimating the body mass of temnospondyls but in consideration of the following caveats. As outlined above, this method overestimated the mass of *Crocodylus porosus* (Fig. 4). This casts

some doubt on the formula's applicability to temnospondyls due to the crocodile-like morphology of many species. Pough (1980) did not provide the dataset or error margin for any of his formulae, which means that a confidence interval cannot be acquired. Furthermore, Pough (1980) stated that the formulae (both TL and SVL) for estimating the mass of salamanders is based on individuals that weighed between 0.03 and 1044 g, which indicates that large taxa would fall out of the model's prediction range. Predictably, Santini *et al.*'s (2018) SVL P equation did not produce accurate estimates in any extant species, as none are paedomorphic (Figs 2–4), but was included here for the sake of completeness.

Farlow *et al.*'s (2005) FC equation delivered mixed signals when predicting the mass of the extant taxa (Figs 2–4). It proved accurate for both aquatic giant salamander species (*Andrias* spp.; Fig. 2), but results were not compelling when applied to the semi-aquatic or terrestrial taxa (Figs 3, 4). When applied to the temnospondyls, the estimate for the presumably aquatic *P. davidi* (172–365 kg) is comparable to those obtained by the two methods discussed above (Fig. 6A), while the estimate for the terrestrial *E. megacephalus* (204–434 kg) is comparatively high (Fig. 6B). Farlow *et al.*'s (2005) equations differ from the others used in this study in that they reflect intraspecific allometric patterns (in *Alligator mississippiensis*). By applying this equation to any other taxon, we must assume that the intraspecific relationship, which is the product of ontogeny (and also potentially includes sexual dimorphism), is the same as the estimated taxon. This assumption is difficult to confirm and likely to be invalid for living amphibians and fossil temnospondyls (Steyer 2000). Accordingly, we include Farlow *et al.*'s (2005) FC equation for the sake of completeness but recommend caution when using it.

Using stylopodial measurements to estimate the body mass of salamanders is potentially problematic due to their unique ability to regenerate limbs. As demonstrated by Bothe *et al.* (2021), regeneration may produce osteological deformations in the limb bones of salamanders, potentially modifying their circumference or length. Furthermore, limb regeneration has also been observed in temnospondyls and could be a primitive tetrapod or even vertebrate feature (Fröbisch *et al.* 2014). Limb-based mass estimation equations, such as those of Farlow *et al.* (2005) and Campione & Evans (2012), could be affected by deformations of the femur and humerus that change the circumference or length of the bones. None of the amphibians in this study shows any osteological deformation of the humerus or femur, suggesting that regeneration is not a factor here. It is important to note that the smallest animal within the extant dataset of Campione & Evans (2012) is a chipmunk, at 53 g. The weight ranges derived from the literature for both *A. tigrinum*

(21–45 g; Fig. 3A) and *T. torosa* (7–14 g; Fig. 3B) (Latimer *et al.* 1961; Feder 1978) are outside of the model's prediction range. The difference between the weight of *A. tigrinum* and the chipmunk in the dataset of Campione & Evans (2012) is not large, and therefore the mass estimation produced is only slightly higher than expected. However, because the weight of *T. torosa* is substantially lower than 53 g, the supporting data are no longer applicable, and the mass of this taxon is significantly overestimated. This method also underestimated the mass of both *Andrias* species, which is unsurprising as this method was developed for terrestrial tetrapods only (Fig. 2). Nonetheless, we assert that Campione & Evans' (2012) stylopodial method applied here is an appropriate model for estimating temnospondyl body mass, especially among terrestrial taxa. Here, the estimations produced by this method align with those produced by other methods that do not rely on limb bones, including the O'Brien *et al.* (2019) and Pough (1980) TL and MCH methods.

Of all methods applied in this study, GDI and MCH are the most time consuming and require specialized equipment (such as 3D scanners and computer modelling software). Both methods require complete skeletons of the taxa in question and involve multiple steps before body mass can be estimated. Our results show that GDI is inaccurate across most comparisons, presumably due to the degree of speculation required to create the soft tissue outline on the silhouettes (see Campione & Evans 2020). The MCH estimations of *C. porosus*, *P. davidi*, and *E. megacephalus* are very similar to the estimations produced by the regression equations applied herein (Figs 4, 5), as was previously asserted by Campione & Evans (2020). However, MCH estimations of the smaller amphibian taxa did not align with the actual masses of the animals in life. This study is the first to use MCH mass estimation for amphibians. As mentioned above, a second set of MCH estimations was produced for the four salamander taxa in this study, combining the head and body into a single functional element, which is more reflective of the appearance of the animal in life. In all but *A. davidianus*, this did not produce widely different results to the first method, where the head and body were treated as separate elements. This highlights a limitation of using MCH, as it is usually impossible to know the extent of soft tissue when working with animals known only from skeletal remains. A related limitation of both MCH and GDI methods is the assumption of the amount of cartilage (and interosseous spacing) in extinct organisms (Campione & Evans 2020), as cartilage (like other soft tissues) is rarely preserved in fossils (Bonnan *et al.* 2010; Tsai & Holliday 2015). Despite this, as the estimation produced did not differ greatly in three of the

four taxa, the utility of MCH as a mass estimation method is still significant.

Although the TL of the *C. porosus* specimen used in this study (210 cm) surpasses that of *E. megacephalus* (192 cm) and is less than *P. davidi* (245 cm), the mass estimates (across all methods) are considerably higher for the temnospondyls. However, the skulls of the temnospondyls are significantly longer, wider, and more robust than that of *C. porosus*. The *C. porosus* used in this study (NENH-RE-00266) is not a full-grown adult (Klinkhamer *et al.* 2017), whereas all other specimens are inferred to be fully developed. This probably influences the mass estimates to some degree, as some skeletal elements may not have been fully developed at the time of the animal's death. Crocodylians are known to continue growing even in maturity (Hutton 1987), so the size that this individual could have attained as an adult is unknown.

Prior to this study, the mass of *Paracyclotosaurus davidi* had not been considered, apart from within Watson's (1958) original description, which stated that 'the weight could be estimated by making a number of assumptions' (p. 253) and that 'roughly the creature is larger than a man in bulk and presumably in weight' (p. 253). Published masses of *Eryops megacephalus* range from 100 to 175 kg (Bakker 1975; Florides *et al.* 2001) but these appear to be rough estimates, not derived from any quantitative method. Other studies suggest that *Eryops* had a large body mass (Miner 1925; Dilkes 2014) but do not give an estimate. Considering the methods above, which give reasonable estimates of the masses of the extant taxa, we propose that *P. davidi* had a body mass of between 159 and 365 kg, and *E. megacephalus* had a body mass between 102 and 222 kg.

CONCLUSION

Estimating the body mass of extinct animals, such as temnospondyls, presents a challenge when there are no living descendants. Here we have found that many established body mass estimation methods provide scope to estimate the mass from both complete and incomplete fossils and thus present an opportunity to estimate body size in a large sample of temnospondyls. It is unlikely that any single method would be universally applicable across the entire clade, due to morphological diversity and inconsistent preservation. However, the O'Brien *et al.* (2019) adjusted HW, Pough (1980) TL, Campione & Evans (2012) HcFc and MCH methods provide a variety of accurate approaches to estimating the body mass of temnospondyls, which can be selected and applied based on the fossils available.

As a highly species-rich clade with a fossil record that extends over 200 million years and across two mass

extinction events (Ruta & Benton 2008), temnospondyls are of great evolutionary interest. As the impacts of body size on morphology, biomechanics and development in temnospondyls have already been observed (Schoch & Fröbisch 2006; Schoch 2013; Fortuny *et al.* 2016), analysis of patterns in body size evolution in this group over time may provide insights into mechanisms which allowed for species diversification and longevity.

Acknowledgements. We thank Egon Heiss (Friedrich Schiller University Jena) and Ada Klinkhamer for allowing us to use their 3D data. Carl Mehling (American Museum of Natural History) provided useful information on the providence of AMNH FR 4657. Damien Germain (Muséum national d'Histoire naturelle) provided measurements of MNHN-F-1957-6 and gave access to the photogrammetry model. Daryl Coldren, Joshua Mata, Alan Resetar (Field Museum) provided measurement, weight data and providence information for FMNH 31536. Thomas Peachey (Australian Museum) assisted in scanning AM F151922 and processing the CT data of THNC 17991 and THNC 19196. Rex Mitchell (Flinders University) assisted in processing the 3D data of AM F151922. LJH is funded under an Australian Government Research Training Program (RTP) Scholarship. NEC is funded under an Australian Research Council Discovery Early Career Research Grant (DE190101423). Alexandra Houssaye and a second, anonymous, referee commented on an earlier draft of this manuscript. Open access publishing facilitated by University of New South Wales, as part of the Wiley - University of New South Wales agreement via the Council of Australian University Librarians.

Author contributions. **Conceptualization** L. J. Hart (LJH), N. E. Campione (NEC), M. R. McCurry (MRM); **Data Curation** LJH, NEC, Damien Germain, Lilian Cazes, Daryl Coldren, Joshua Mata, Alan Resetar, Egon Heiss, Matthew Corbett; **Formal Analysis** LJH, NEC, MRM; **Funding Acquisition** LJH, NEC, MRM; **Investigation** LJH, NEC, MRM; **Methodology** LJH, NEC, MRM; **Project Administration** LJH; **Resources** LJH, MRM; **Supervision** MRM; **Validation** LJH, NEC; **Visualization** LJH; **Writing – Original Draft Preparation** LJH; **Writing – Review & Editing** LJH, NEC, MRM.

DATA ARCHIVING STATEMENT

Data for this study, including volumetric models and scan data are available in MorphoSource (<https://www.morphosource.org/projects/000445986>) and the Dryad Digital Repository (<https://doi.org/10.5061/dryad.zcrjdfnfd>). Individual specimen data packages are: 1/2009, <https://doi.org/10.17602/M2/M446021>; NENH-RE-00266, <https://doi.org/10.17602/M2/M446000>; AM F151922, <https://doi.org/10.17602/M2/M445991>; MNHN-F-1957-6, <https://doi.org/10.17602/M2/M445996>.

Editor. Marcello Ruta

REFERENCES

- ANDERSON, J. F., HALL-MARTIN, A. and RUSSELL, D. A. 1985. Long-bone circumference and weight in mammals, birds and dinosaurs. *Journal of Zoology*, **207**, 53–61.
- ATKINS, J. B., REISZ, R. R. and MADDIN, H. C. 2019. Braincase simplification and the origin of lissamphibians. *PLoS One*, **14**, e0213694.
- BAKKER, R. T. 1975. Dinosaur renaissance. *Scientific American*, **232**, 58–79.
- BENSON, R. B., CAMPIONE, N. E., CARRANO, M. T., MANNION, P. D., SULLIVAN, C., UPCHURCH, P. and EVANS, D. C. 2014. Rates of dinosaur body mass evolution indicate 170 million years of sustained ecological innovation on the avian stem lineage. *PLoS Biology*, **12**, e1001853.
- BENSON, R. B., HUNT, G., CARRANO, M. T. and CAMPIONE, N. 2018. Cope's rule and the adaptive landscape of dinosaur body size evolution. *Paleontology*, **61**, 13–48.
- BONNAN, M. F., SANDRIK, J. L., NISHIWAKI, T., WILHITE, D. R., ELSEY, R. M. and VITTORE, C. 2010. Calcified cartilage shape in archosaur long bones reflects overlying joint shape in stress-bearing elements: implications for nonavian dinosaur locomotion. *Anatomical Record*, **293**, 2044–2055.
- BOTHE, V., MAHLOW, K. and FRÖBISCH, N. B. 2021. A histological study of normal and pathological limb regeneration in the Mexican axolotl *Ambystoma mexicanum*. *Journal of Experimental Zoology B*, **336**, 116–128.
- BRASSEY, C. A. 2017. Body mass estimation in paleontology: a review of volumetric techniques. *The Paleontological Society Papers*, **22**, 133–156.
- BRASSEY, C. A. and SELLERS, W. I. 2014. Scaling of convex hull volume to body mass in modern primates, non-primate mammals and birds. *PLoS One*, **9**, e91691.
- BRASSEY, C. A., MAIDMENT, S. C. and BARRETT, P. M. 2015. Body mass estimates of an exceptionally complete *Stegosaurus* (Ornithischia: Thyreophora): comparing volumetric and linear bivariate mass estimation methods. *Biology Letters*, **11**, 20140984.
- BRASSEY, C. A., O'MAHONEY, T. G., KITCHENER, A. C., MANNING, P. L. and SELLERS, W. I. 2016. Convex-hull mass estimates of the dodo (*Raphus cucullatus*): application of a CT-based mass estimation technique. *PeerJ*, **4**, e1432.
- BROWN, J. H., GILLOOLY, J. F., ALLEN, A. P., SAVAGE, V. M. and WEST, G. B. 2004. Toward a metabolic theory of ecology. *Ecology*, **85**, 1771–1789.
- BROWNE, R., LI, H., WANG, Z., OKADA, S., HIME, P., McMILLAN, A., WU, M., DIAZ, R., McGINNITY, D. and BRIGGLER, J. 2014. The giant salamanders (Cryptobranchidae): Part B. Biogeography, ecology and reproduction. *Amphibian & Reptile Conservation*, **5**, 30–50.
- BURNESS, G. P., DIAMOND, J. and FLANNERY, T. 2001. Dinosaurs, dragons, and dwarfs: the evolution of maximal body size. *Proceedings of the National Academy of Sciences*, **98**, 14518–14523.
- CAMPIONE, N. E. 2017. Extrapolating body masses in large terrestrial vertebrates. *Paleobiology*, **43**, 693–699.

- CAMPIONE, N. E. 2020. MASSTIMATE: Body mass estimation equations for vertebrates. R Package v2.0-1. <https://cran.r-project.org/web/packages/MASSTIMATE/index.html>
- CAMPIONE, N. E. and EVANS, D. C. 2012. A universal scaling relationship between body mass and proximal limb bone dimensions in quadrupedal terrestrial tetrapods. *BMC Biology*, **10**, 60.
- CAMPIONE, N. E. and EVANS, D. C. 2020. The accuracy and precision of body mass estimation in non-avian dinosaurs. *Biological Reviews*, **95**, 1759–1797.
- CAMPIONE, N. E., EVANS, D. C., BROWN, C. M. and CARRANO, M. T. 2014. Body mass estimation in non-avian bipeds using a theoretical conversion to quadruped stylopodial proportions. *Methods in Ecology & Evolution*, **5**, 913–923.
- CHERNIN, S. 1970. Capitosaurid amphibians from the upper Luangwa Valley, Zambia. *Palaeontologia Africana*, **7**, 33–55.
- CODRON, D., CARBONE, C., MÜLLER, D. W. and CLAUSS, M. 2012. Ontogenetic niche shifts in dinosaurs influenced size, diversity and extinction in terrestrial vertebrates. *Biology Letters*, **8**, 620–623.
- COPE, E. D. 1877. Descriptions of extinct Vertebrata from the Permian and Triassic formations of the United States. *Proceedings of the American Philosophical Society*, **17** (100), 182–193.
- DAMIANI, R. J. 2008. A systematic revision and phylogenetic analysis of Triassic mastodonsauroids (Temnospondyli: Stereospondyli). *Zoological Journal of the Linnean Society*, **133**, 379–482.
- DIGIMORPH STAFF. 2008a. *Ambystoma tigrinum*, tiger salamander. *Digital Morphology*. http://digimorph.org/specimens/Ambystoma_tigrinum/whole/ [accessed 16 November 2021]
- DIGIMORPH STAFF. 2008b. *Taricha torosa*, California newt. *Digital Morphology*. http://digimorph.org/specimens/Taricha_torosa/whole/ [accessed 16 November 2021]
- DILKES, D. 2014. Carpus and tarsus of Temnospondyli. *Vertebrate Anatomy Morphology Palaeontology*, **1**, 51–87.
- FARLOW, J. O., HURLBURT, G. R., ELSEY, R. M., BRITTON, A. R. and LANGSTON, J. R. W. 2005. Femoral dimensions and body size of *Alligator mississippiensis*: estimating the size of extinct mesoeucrocodylians. *Journal of Vertebrate Paleontology*, **25**, 354–369.
- FEDER, M. E. 1978. Environmental variability and thermal acclimation in neotropical and temperate zone salamanders. *Physiological Zoology*, **51**, 7–16.
- FLACKE, G. L. and DECHER, J. 2019. *Choeropsis liberiensis* (Artiodactyla: Hippopotamidae). *Mammalian Species*, **51**, 100–118.
- FLORIDES, G. A., KALOGIROU, S. A., TASSOU, S. A. and WROBEL, L. 2001. Natural environment and thermal behaviour of *Dimetrodon limbatus*. *Journal of Thermal Biology*, **26**, 15–20.
- FORTUNY, J., MARCÉ-NOGUÉ, J., DE ESTEBAN-TRIVIGNO, S., GIL, L. and GALOBART, À. 2011. Temnospondyli bite club: ecomorphological patterns of the most diverse group of early tetrapods. *Journal of Evolutionary Biology*, **24**, 2040–2054.
- FORTUNY, J., MARCÉ-NOGUÉ, J., HEISS, E., SANCHEZ, M., GIL, L. and GALOBART, À. 2015. 3D bite modeling and feeding mechanics of the largest living amphibian, the Chinese giant salamander *Andrias davidianus* (Amphibia: Urodela). *PLoS One*, **10**, e0121885.
- FORTUNY, J., MARCÉ-NOGUÉ, J., STEYER, J., DE ESTEBAN-TRIVIGNO, S., MUJAL, E. and GIL, L. 2016. Comparative 3D analyses and palaeoecology of giant early amphibians (Temnospondyli: Stereoospondyli). *Scientific Reports*, **6**, 1–10.
- FRÖBISCH, N. B., BICKELMANN, C. and WITZMANN, F. 2014. Early evolution of limb regeneration in tetrapods: evidence from a 300-million-year-old amphibian. *Proceedings of the Royal Society B*, **281**, 20141550.
- GILLOOLY, J. F., BROWN, J. H., WEST, G. B., SAVAGE, V. M. and CHARNOV, E. L. 2001. Effects of size and temperature on metabolic rate. *Science*, **293**, 2248–2251.
- GRADY, J. M., ENQUIST, B. J., DETTWEILER-ROBINSON, E., WRIGHT, N. A. and SMITH, F. A. 2014. Evidence for mesothermy in dinosaurs. *Science*, **344**, 1268–1272.
- HART, L. 2022a. Dataset for: On the estimation of body mass in temnospondyls: a case study using the large bodied Eryops and Paracyclotosaurus. *Dryad Digital Repository*. <https://doi.org/10.5061/dryad.zcrjdfnfd>
- HART, L. 2022b. Temnospondyls, crocodiles and amphibians. *MorphoSource*. <https://www.morphosource.org/projects/000445986>
- HEISS, E., NATCHEV, N., GUMPENBERGER, M., WEISSENBACHER, A. and VAN WASSENBERGH, S. 2013. Biomechanics and hydrodynamics of prey capture in the Chinese giant salamander reveal a high-performance jaw-powered suction feeding mechanism. *Journal of the Royal Society Interface*, **10**, 20121028.
- HENDERSON, D. M. 1999. Estimating the masses and centers of mass of extinct animals by 3-D mathematical slicing. *Paleobiology*, **25**, 88–106.
- HURLBURT, G. 1999. Comparison of body mass estimation techniques, using recent reptiles and the pelycosaur *Edaphosaurus boanerges*. *Journal of Vertebrate Paleontology*, **19**, 338–350.
- HUTCHINSON, J. R., NG-THOW-HING, V. and ANDERSON, F. C. 2007. A 3D interactive method for estimating body segmental parameters in animals: application to the turning and running performance of *Tyrannosaurus rex*. *Journal of Theoretical Biology*, **246**, 660–680.
- HUTTON, J. M. 1987. Growth and feeding ecology of the Nile crocodile *Crocodylus niloticus* at Ngezi, Zimbabwe. *Journal of Animal Ecology*, **56**, 25–38.
- JENKINS, F. A. Jr, SHUBIN, N. H., GATESY, S. M. and WARREN, A. 2008. *Gerrothorax pulcherrimus* from the Upper Triassic Fleming Fjord Formation of East Greenland and a reassessment of head lifting in temnospondyl feeding. *Journal of Vertebrate Paleontology*, **28**, 935–950.
- KLINKHAMER, A. J., WILHITE, D. R., WHITE, M. A. and WROE, S. 2017. Digital dissection and three-dimensional interactive models of limb musculature in the Australian estuarine crocodile (*Crocodylus porosus*). *PLoS One*, **12**, e0175079.
- LARRAMENDI, A., PAUL, G. S. and HSU, S. Y. 2020. A review and reappraisal of the specific gravities of present and past multicellular organisms, with an emphasis on tetrapods. *Anatomical Record*, **304**, 1833–1888.

- LATIMER, H. B., ROOFE, P. G. and FENG, L. S. 1961. Weights and linear measurements of the body and of some organs of the tiger salamander. *Anatomical Record*, **141**, 35–44.
- LAURIN, M. and REISZ, R. R. 1997. A new perspective on tetrapod phylogeny. 9–59. In SUMIDA, S. S. and MARTIN, K. L. M. (eds) *Amniote origins: Completing the transition to land*. Academic Press.
- LAURIN, M. and REISZ, R. R. 1999. A new study of *Solenodonsaurus janenschi*, and a reconsideration of amniote origins and stegocephalian evolution. *Canadian Journal of Earth Sciences*, **36**, 1239–1255.
- LIU, C. 1950. *Amphibians of western China*. Fieldiana: Zoology Memoirs, **2**. Chicago Natural History Museum.
- MARJONIVIĆ, D. and LAURIN, M. 2013. The origin(s) of extant amphibians: a review with emphasis on the “lepospondyl hypothesis”. *Geodiversitas*, **35**, 207–272.
- MILNER, A. R. 1988. The relationships and origin of living amphibians. 59–102. In BENTON, M. J. (ed.) *The phylogeny and classification of the tetrapods*. Vol. 1. *Amphibians, reptiles and birds*. Oxford University Press.
- MILNER, A. R. 1993. The Paleozoic relatives of lissamphibians. *Herpetological Monographs*, **7**, 8–27.
- MINER, R. W. 1925. The pectoral limb of *Eryops* and other primitive tetrapods. *Bulletin of the American Museum of Natural History*, **51**, art. 7.
- MOTANI, R. 2001. Estimating body mass from silhouettes: testing the assumption of elliptical body cross-sections. *Paleobiology*, **27**, 735–750.
- O'BRIEN, H. D., LYNCH, L. M., VLIET, K. A., BRUEGEN, J., ERICKSON, G. M. and GIGNAC, P. M. 2019. Crocodylian head width allometry and phylogenetic prediction of body size in extinct crocodyliforms. *Integrative Organismal Biology*, **1**, obz006.
- PAWLEY, K. and WARREN, A. 2006. The appendicular skeleton of *Eryops megacephalus* Cope, 1877 (Temnospondyli: Eryopoidea) from the Lower Permian of North America. *Journal of Paleontology*, **80**, 561–580.
- PIERSON, T. W., KIERAN, T. J., CLAUSE, A. G. and CASTLEBERRY, N. L. 2020. Preservation-induced morphological change in salamanders and failed DNA extraction from a decades-old museum specimen: implications for *Plethodon ainsworthi*. *Journal of Herpetology*, **54**, 137–143.
- POUGH, F. H. 1980. The advantages of ectothermy for tetrapods. *The American Naturalist*, **115**, 92–112.
- R CORE TEAM. 2013. R: A language and environment for statistical computing. R Foundation for Statistical Computing. <https://www.R-project.org>
- REIF, J. S., BACHAND, A., AGUIRRE, A. A., BORJESSON, D. L., KASHINSKY, L., BRAUN, R. and ANTONELIS, G. 2004. Morphometry, hematology, and serum chemistry in the Hawaiian monk seal (*Monachus schauinslandi*). *Marine Mammal Science*, **20**, 851–860.
- ROVINSKY, D. S., EVANS, A. R., MARTIN, D. G. and ADAMS, J. W. 2020. Did the thylacine violate the costs of carnivory? Body mass and sexual dimorphism of an iconic Australian marsupial. *Proceedings of the Royal Society B*, **287**, 20201537.
- RUTA, M. and BENTON, M. J. 2008. Calibrated diversity, tree topology and the mother of mass extinctions: the lesson of temnospondyls. *Palaeontology*, **51**, 1261–1288.
- RUTA, M. and COATES, M. I. 2007. Dates, nodes and character conflict: addressing the Lissamphibian origin problem. *Journal of Systematic Palaeontology*, **5**, 69–122.
- SANTINI, L., BENITEZ-LOPEZ, A., FICETOLA, G. F. and HUIJBREGTS, M. A. J. 2018. Length-mass allometries in amphibians. *Integrative Zoology*, **13**, 36–45.
- SCHOCH, R. R. 2009. Evolution of life cycles in early amphibians. *Annual Review of Earth & Planetary Sciences*, **37**, 135–162.
- SCHOCH, R. R. 2013. How body size and development biased the direction of evolution in early amphibians. *Historical Biology*, **25**, 155–165.
- SCHOCH, R. R. 2019. The putative lissamphibian stem-group: phylogeny and evolution of the dissorophoid temnospondyls. *Journal of Paleontology*, **93**, 137–156.
- SCHOCH, R. R. and FRÖBISCH, N. 2006. Metamorphosis and neoteny: alternative pathways in an extinct amphibian clade. *Evolution*, **60**, 1467–1475.
- SCHOCH, R. R. and MILNER, A. R. 2004. Structure and implications of theories on the origin of lissamphibians. 345–377. In ARRATIA, G., WILSON, M. V. H. and CLOUTIER, R. (eds) *Recent advances in the origin and early radiation of vertebrates*. Verlag Friedrich Pfeil.
- SCHOCH, R. R. and WITZMANN, F. 2012. Cranial morphology of the plagiosaurid *Gerrothorax pulcherrimus* as an extreme example of evolutionary stasis. *Lethaia*, **3**, 371–385.
- SCHROEDER, K., LYONS, S. K. and SMITH, F. A. 2021. The influence of juvenile dinosaurs on community structure and diversity. *Science*, **371**, 941–944.
- SELLERS, W., HEPWORTH-BELL, J., FALKINGHAM, P., BATES, K., BRASSEY, C., EGERTON, V. and MANNING, P. 2012. Minimum convex hull mass estimations of complete mounted skeletons. *Biology Letters*, **8**, 842–845.
- SEYMOUR, R. S., GIENGER, C., BRIEN, M. L., TRACY, C. R., MANOLIS, S. C., WEBB, G. J. and CHRISTIAN, K. A. 2013. Scaling of standard metabolic rate in estuarine crocodiles *Crocodylus porosus*. *Journal of Comparative Physiology B*, **183**, 491–500.
- SMITH, F. A., LYONS, S. K., ERNEST, S. M., JONES, K. E., KAUFMAN, D. M., DAYAN, T., MARQUET, P. A., BROWN, J. H. and HASKELL, J. P. 2003. Body mass of late Quaternary mammals. *Ecology*, **84**, 3403.
- STEYER, J.-S. 2000. Ontogeny and phylogeny in temnospondyls: a new method of analysis. *Zoological Journal of the Linnean Society*, **130**, 449–467.
- SULEJ, T. and MAJER, D. 2005. The temnospondyl amphibian *Cyclotosaurus* from the Upper Triassic of Poland. *Palaeontology*, **48**, 157–170.
- TRUEB, L. and CLOUTIER, R. 1991. A phylogenetic investigation of the inter-and intrarelationships of the Lissamphibia (Amphibia: Temnospondyli). 223–313. In SCHULTZE, H.-P. and TRUEB, L. (eds) *Origins of the higher groups of tetrapods, controversy and consensus*. Cornell University Press.

- TSAI, H. P. and HOLLIDAY, C. M. 2015. Articular soft tissue anatomy of the archosaur hip joint: structural homology and functional implications. *Journal of Morphology*, **276**, 601–630.
- VAN HETEREN, A. H., VAN DIERENDONCK, R. C., VAN EGMOND, M. A., SJANG, L. and KREUNING, J. 2017. Neither slim nor fat: estimating the mass of the dodo (*Raphus cucullatus*, Aves, Columbiformes) based on the largest sample of dodo bones to date. *PeerJ*, **5**, e4110.
- WATSON, D. M. S. 1958. A new labyrinthodont (*Paracyclotosaurus*) from the Upper Trias of New South Wales. *Bulletin of the British Museum of Natural History, London (Geology)*, **3**, 233–263.
- WITMER, L. M. 1995. The extant phylogenetic bracket and the importance of reconstructing soft tissues in fossils. 19–33. In THOMASON, J.J. (ed.) *Functional morphology in vertebrate paleontology*. Cambridge University Press.
- WITZMANN, F. and BRAINERD, E. 2017. Modeling the physiology of the aquatic temnospondyl *Archegosaurus decheni* from the early Permian of Germany. *Fossil Record*, **20**, 105–127.